J Nanostruct 13(4): 1142-1149, Autumn 2023

RESEARCH PAPER

# Effect of Green Synthesis of the ZnO/Ag Nanocomposites on MCF-7 Cancerous Line Using High Content Screening

*Sura Hassan Hamad *, Nedhal Ibrahim Iateff, Ashwaq Talib Hameed*

*College of Education for women, University of Anbar, Iraq*

ARTICLE INFO

***Article History:***
*Received 11 June 2023*
*Accepted 17 September 2023*
*Published 01 October 2023*

***Keywords:***
*Green*
*MCF-7*
*Nanocomposites*
*Zinc oxide*

ABSTRACT

This research was conducted to evaluate the cytotoxicity of Ag:ZnO nanocomposites prepared from *C. murale* leaves extract on MCF-7 cancer cell line . Four concentrations of 200, 100, 50 and 25 µg/ml were prepared, as the Ag:ZnO Nanocomposites showed the best percentage. Inhibition of the growth of MCF-7 cancer cells. This test included evaluating the effect of Ag:ZnO nanocomposites on the morphology of MCF-7 cancer cells, by detecting changes that occur to cells to measure some cellular indicators including cell permeability, cell number, nuclear content of cells, mitochondrial membrane permeability, and the level of cytochrome C release from cells. The results showed a clear decrease in the number of cells, an increase in nuclear density when the cells were treated with the complex at concentrations of 200 and 100 mg/ml, a significant decrease in the strength of the mitochondrial membrane, and an increase in cytochrome C levels at concentrations 200 and 100 µg/ml, and the results showed the ability of the complex to increase the permeability of the cell membrane. For cells at a concentration of 200 mg/ml because of the damage that occurs in the cell membrane, which leads to an increase in the permeability of cell membranes.

**How to cite this article**
*Hamad S., Iateff N., Hameed A. Effect of Green Synthesis of the ZnO/Ag Nanocomposites on MCF-7 Cancerous Line Using High Content Screening. J Nanostruct, 2023; 13(4):1142-1149. DOI: 10.22052/JNS.2023.04.022*

## INTRODUCTION

Cancer is an incurable disease that causes cells to grow abnormally, and cells multiply and divide irregularly, allowing these cells to spread and divide out of control. Changes in the cell cycle that control oncogenes and tumor suppressor genes lead to the expression of uncontrolled proteins. Natural contributes to stimulating cell division and survival. Cancer is not a single disease, but rather it represents a group of diseases that are characterized by an uncontrolled increase and spread of abnormal cells, and the spread of these cells is uncontrollable. Which leads to death due to a lack of control over the spread of malignant cancer cells. The statistics in Iraq also showed an alarmingly high rate of cancer , due to carcinogenic factors and the environment represented by pollution and radiation. Studies have revealed recent data recorded for cancer in Iraq on the presence of increased rates of cancer and congenital malformations in the city of Fallujah due to the city's exposure to military operations and the use of radioactive materials [1,2]. Nanobiotechnology is the most promising field for the synthesis of new types of particles and can be used in medical and biological applications. Because nanoparticles (NPs) have the potential to bind to the acidic environment that characterizes

* *Corresponding Author Email: sur20w4005@uoanbar.edu.iq*

tumor tissues, it is believed that selective targeting strategies using nanoparticles (NPs) facilitate more effective cancer detection and treatment while reducing the side effects of healthy cells [3]. High Content Screening device. (HCS) is a system that automatically measures the intensity and location of intracellular and intracellular signals [4], and HCS provides a multifaceted analysis of the toxicity of compounds at the individual cell level [5] and [6]. This technique measures the intensity and location of the glow signals within the single-cell and the cellular components between the collected cells, where a timely imaging analysis is performed as they reach the fluorescence channels. Fluorescence immunocytochemistry and variation in cellular morphology and intracellular trafficking and other changes [7,8], NPs have been investigated in relation to their various cytotoxic effects using photostimulation in human malignant melanoma (HT144) and normal cells in human colonic epithelial tissue (HCEC), where it showed that zinc and silver nanocomposites have an effective effect in killing cancer cells more efficiently than they severely affect normal cells during detection through the spectrophotometer.

*C. murale* plant of the family Chenopodiaceae and formerly called Amaranthaceae is a rich source of many bioactive compounds [9], a winter herb that naturally grows along roadsides and is cultivated fields and contains a number of active substances. Which is characterized active against pathogens such as fungi and pathogenic bacteria and is used in many medical applications such as hepatoprotective drugs, analgesics, and antihypertensive drugs [10]. Vitality against tumors and pathogenic microorganisms. The study aimed to prepare and test the silver-zinc nanocomposite and test its effect against MCF-7 cancerous line using High Content Screening.

## MATERIALS AND METHODS

### *Collection of plant samples*

The leaves of C. murale were collected from central Ramadi / Iraq and were prepared and dried according to the instructions followed in [8], and the plant was classified by Dr. Ashwaq Taleb Hameed - College of Education. For Women - Medical Herb.

### *Preparation of silver-zinc nanocomposite*

An alcoholic extract was prepared with a saxolites device, according to the protocol [11], 25 ml of C. murale extract was added at a concentration of 1 mg/ml to the mixture of minerals, both separately, with stirring for an hour, and the color shift was observed and then worked for it. Centrifuge and wash the precipitate with ethanol and distilled water several times and then

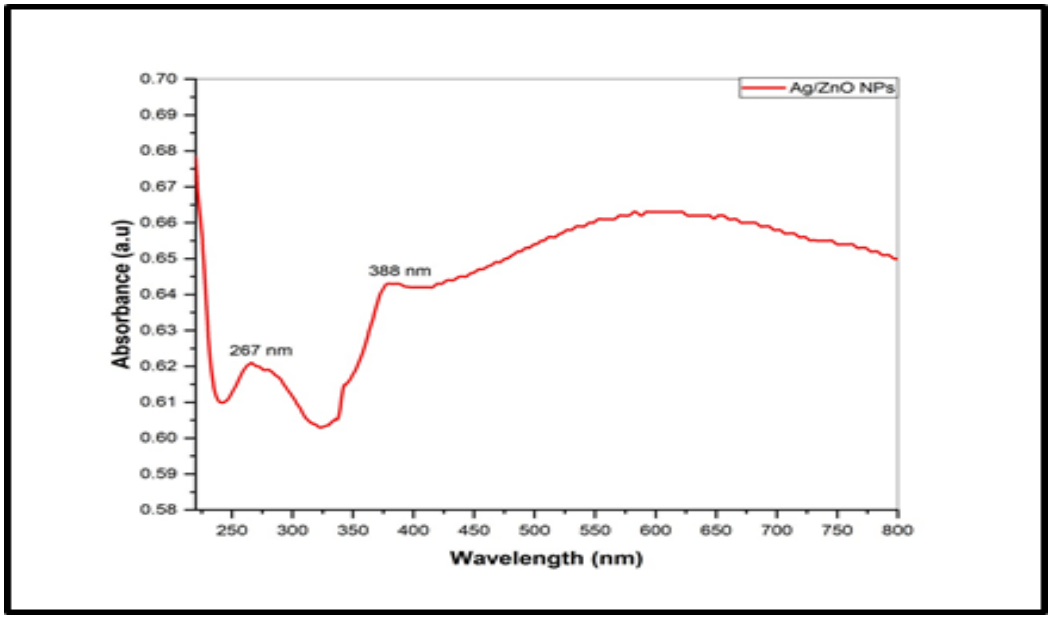


Fig. 1. UV absorption spectrum of Ag:ZnO nanoparticles from 200 nm to 1000 nm.

dried at 60 °C for 4 hours [12], an equal amount of ZnO and Ag NPs dissolved in ethanol was mixed and the mixture was mixed on a magnetic stirrer for 1 h. At a temperature of 60 ° C for one hour, four concentrations of 200, 100, 50, and 25 micrograms/ml were prepared.

*High Content Screening (HCS)*

This assay for the purpose of studying the effect of nanoparticles manufactured from the alcoholic extract of *C. murale* on breast cancer cells MCF-7 are cancer cells isolated from a 69-year-old Caucasian woman in 1970 with breast cancer, MCF-7 is an acronym for the Michigan Cancer Foundation 7- Where a cell line was established in 1973 AD by Herbert Soule and his colleagues [13], this test included measuring and monitoring the changes that occur in cell nuclei, cell membrane

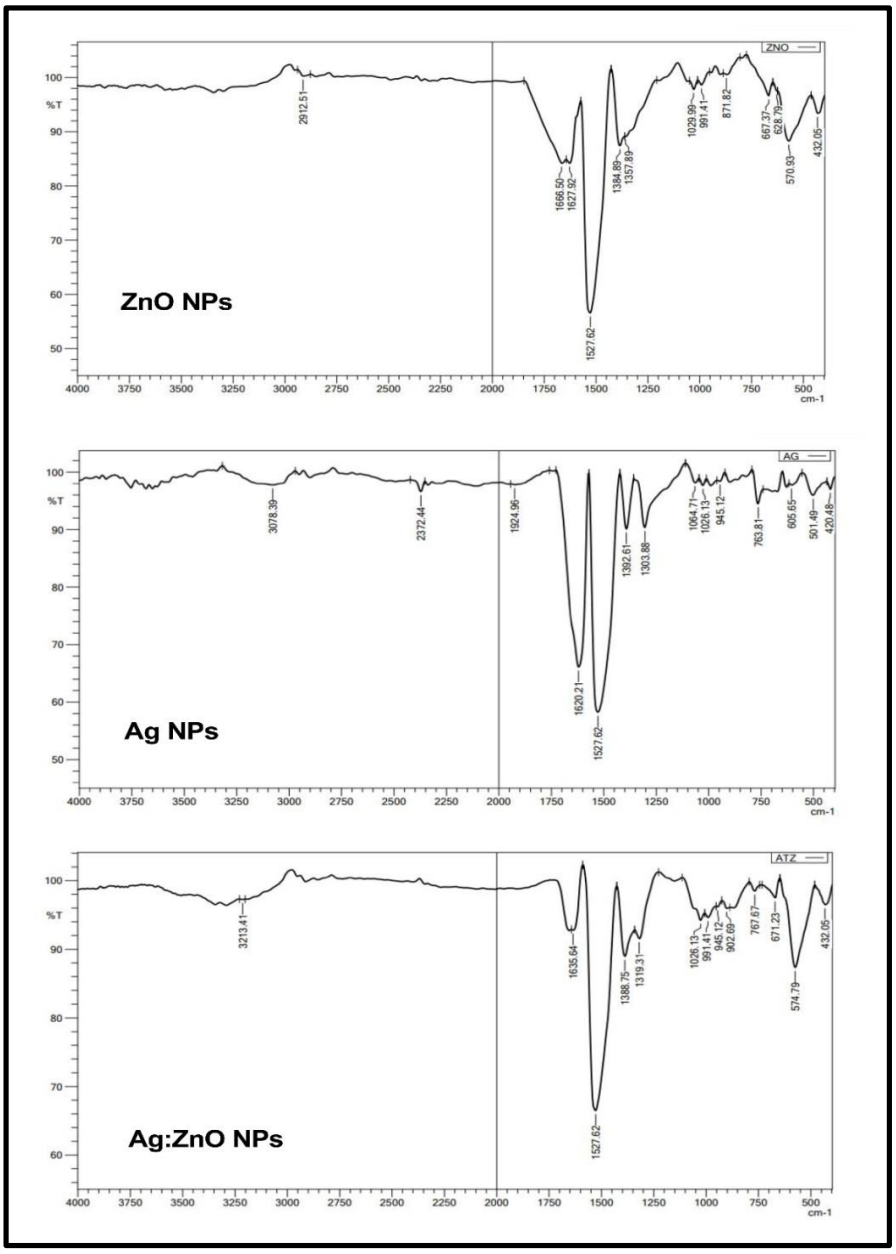


Fig. 2. FT-IR absorption spectrum of ZnO, Ag, and Ag: ZnO nanocomposite particles from 500 nm to 4000 $cm^{-1}$.

permeability, and release of cytochrome from mitochondria. This test was carried out at the University of Malaya / Department of Pharmacology / Center for Investigation of New Drugs in Malaysia. Cancer cell line cells were prepared as mentioned in [12], placed on a plate (96 holes), and incubated in a 5% CO2 incubator at a temperature of 37 °C for 24 h. , 50 µl of concentrations of nanoparticles manufactured from the alcoholic extract C. murale 200, 100, 50, and 25 µg/ml were added to each hole and three holes for each concentration, while 50µl of culture medium was added to the control hole. 50µl of live-cell dye was added to each hole and incubated for 30 minutes at a temperature of 37 °C· and incubated for 10 minutes at room temperature away from light· The plate was washed twice with 100µl of the washing solution for 10 minutes, then 100µl of blocking buffer was added to each hole and incubated for 15 minutes at room temperature. After removing the blocking solution, 50µl of the primary antibody solution was added to each hole. And incubated for one hour at room temperature 25 °C in the dark, 50 µl of dye solution secondary antibodies were added and incubated for one hour at room temperature away from light, then the dye solution was discarded after incubation and washed with water, 100 µl/hole was added of washing buffer solution and then take the plate to read it using Array Scan HCS Reader

## RESULTS AND DISCUSSION

In Fig. 1 sharp absorbance at a wavelength of 388 nm was obsorved due to the strong coupling between ZnO and Ag nanoparticles, the surface plasmon range of Ag:ZnO nanocomposite is clearly wider. Highest light temperature: ZnO for light at a peak at the wavelength of 267nm indicative of the highest *C. murale* extract and a perfect correlation between plant extract and silver oxide and silver nanoparticles after reduction. It has been shown that silver nanoparticles with a size of 10-50 nm embedded in oxide nanoparticles add to a direct light spike [14].

The FT-IR spectrum of Ag:ZnO nanocomposite were recorded in the range 500-4000 $cm^{-1}$, the beam at 574.8 $cm^{-1}$ and 763 $cm^{-1}$ indicates the bonds of Zn-O and Ag-O groups respectively (Fig. 2). A peak was determined at the 1527.62 $cm^{-1}$ band in ZnO nanoparticles and a peak at the same band in silver nanoparticles was determined which is attributed to the C=C aromatic bonds. As for the

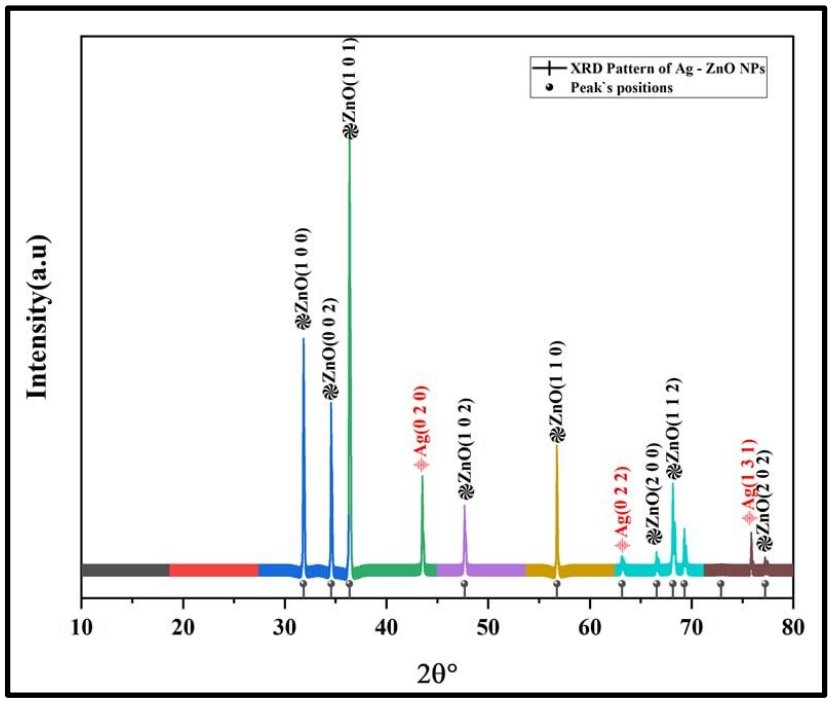


Fig. 3. X-ray diffraction patterns of silver and zinc nanocomposite prepared from C. murale extract after 24 h.

state of Ag:ZnO nanocomposite after the binding of zinc oxide nanoparticles with silver particles, it was detected after the intensity of the absorbance peak decreased between 1600-2750 $cm^{-1}$ due to the binding of Ag nanoparticles on the surface of the ZnO nanoparticles [15].

XRD was also used to analyze the crystal shape and size of the Ag:ZnO nanocomposite, the results of the XRD analysis of the complex particles prepared from *C. murale* extract showed diffraction peaks at = 31.86°, 34.58°, 36.38°, 43.53°, 47.71°, 56.76, 63.2, 66.6, 68.2, 69.32,

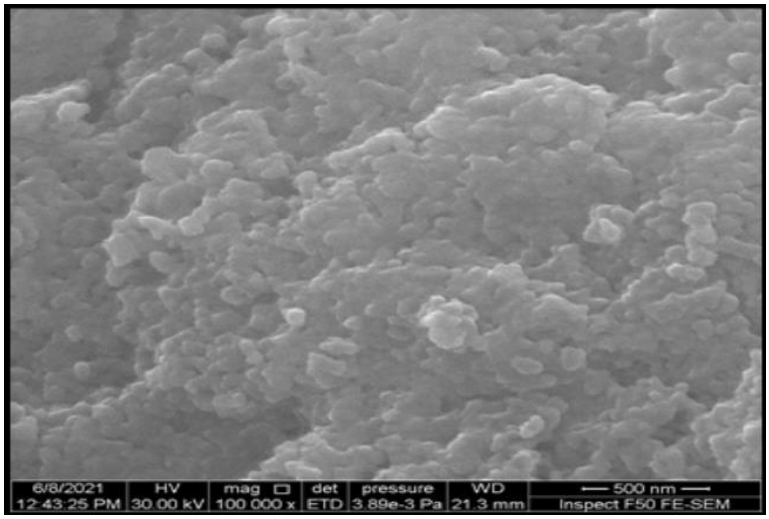


Fig. 4. The shape of the Ag: ZnO nanocomposite under a scanning electron microscope,the magnification power is 100,000X.

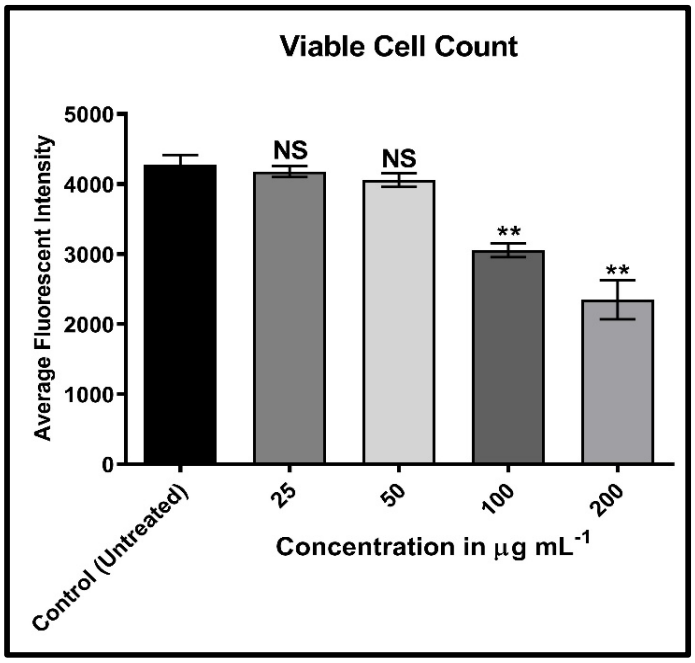


Fig. 5. Effect of Ag: ZnO nanocomplex concentrations on the viability of MCF-7 cells after 24 hours of incubation at 37 °C using HCS device.

75.88, and 77.36°, respectively. (Fig. 3). When comparing the diffraction degrees of the complex with the diffraction degrees of both zinc oxide and silver nanoparticles, it showed the presence of two different sets of diffraction peaks, which indicates the binding of both zinc oxide and silver in one complex [16]. The average size of silver nanoparticles was calculated to be 43.09 nm.

The results are shown in the Fig. 4 the size and shape of the surfaces of the Ag: ZnO nanocomposite, SEM images show nanocomposite in the form of irregularly shaped clumps or at most hexagons or cubes. The appearance of the complex nanoparticles in this way is due to the presence of silver particles bound with zinc oxide particles. In addition, the presence of pores in the information gives clear evidence that AgNPs are encapsulated on the surface of ZnO [17]. The average nanocomposite diameter was calculated, which was 50.4nm.

The results shown in Fig. 5 show that the Ag:ZnO nanocomposite has high cytotoxicity to the MCF-7 cancer line cells at the concentration of 200 and 100 mg/ml with a significant difference

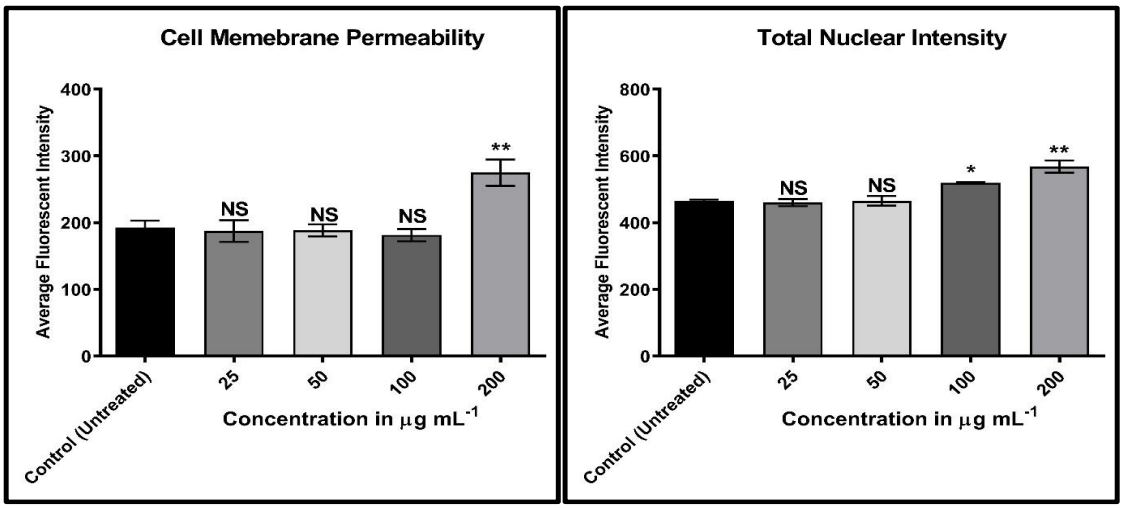


Fig. 6. Effect of Ag:ZnO nanocomplex concentrations on nuclear density (right) and cell membrane (left) of MCF-7 cells after 24 hours of incubation at 37 °C using HCS apparatus.

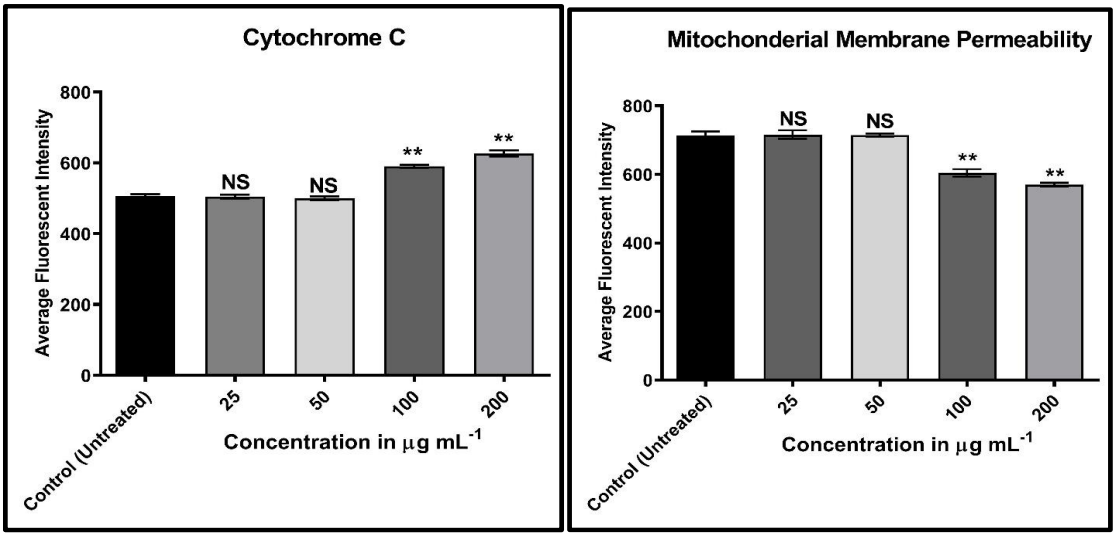


Fig. 7. Effect of different concentrations of Ag:ZnO nanocomposite on mitochondrial membrane permeability (right) and cell membrane (left) of MCF-7 cells after 24 hours of incubation at 37°C using HCS apparatus

($p \leq 0.01$) compared to the control cells , where the nanocomposite treatment led At these concentrations, a clear decrease in the number of cells was shown in Fig. 5, while the concentrations of 50 and 25 mg/ml did not indicate any significant differences (Fig. 5). The results also showed the ability of the complex to increase the permeability of the cell membranes with a significant difference ($p \leq 0.01$) at a concentration of 200 mg/ml due to the damages that occur in the cell membrane of cells and leading to an increase in the permeability of cell membranes, and there is no such effect in other concentrations on membrane permeability. (Fig. 6). An increase in nuclear density was observed when the cells were treated with the complex at concentrations of 200 and 100 mg/ml with a significant difference ($p \leq 0.01$) compared to the control treatment cells, while for the rest of the concentrations, no effect was shown on the level of nuclear density of cells compared to the control treatment (Fig. 7). The fourth indicator studied is mitochondrial membrane strength as an important characteristic of mitochondrial integrity, and membrane depolarization is an ideal indicator of mitochondrial dysfunction that is increasingly affected by drug toxicity and is an effective characterization of cell death signals [18]. The results of Fig. 8 show that the nanocomposite concentrations of 200 and 100 µg/ml caused a significant decrease in mitochondrial membrane strength ($p \leq 0.01$) compared to the control. The results of this indicator showed that there was no significant difference in the strength of the mitochondrial membrane when treated with B at concentrations of 50 and 25 µg/ml.

Cytochrome C is known as a major component of the weakly bound electron transport chain on the outer layer of the inner mitochondrial membrane, and cytochrome c plays a role mainly in programmed cell death [19]. The results (Fig. 7) showed that there were no significant differences between the concentration of 50 µg/ml and the concentration of 25 µg/ml compared to the control. It was also noted that the levels of Cytochrome C increased significantly ($p \leq 0.01$) than the control model at the concentrations of 200 and 100 µg/ml. From the above, it is noted that high concentrations of the complex affect all cellular indicators of the MCF-7 cancer cell line when exposed to the complex for 24 hours at a temperature of 37 °C, which leads to inducing the cells to enter into the process of programmed cell death (Fig. 6). The distinguishing features of the early stages of programmed cell death include disruption of mitochondrial activity and changes in the permeability of their membranes and the redox system within them, which in turn leads to the opening of the membrane pores and allowing

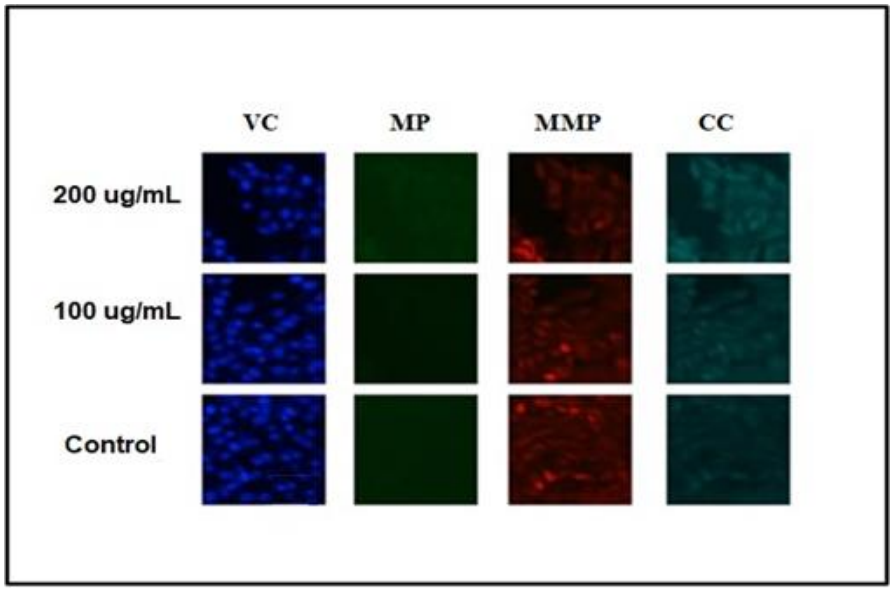


Fig. 8. Effect of Ag:ZnO nanocomposite on nuclear content, cell membrane permeability, mitochondrial membrane permeability, and cytochrome c release level of MCF-7 cancer line cells after incubation for 24 h. at a temperature of 37 °C.

the passage of ions and small molecules through the membrane. The process of opening pores in the cell membrane leads to ionic balance, which in turn leads to the separation of the respiratory chain and the release of cytochrome C into the cell [20].

The use of the cytotoxicity test for drugs is an essential part of detecting new drugs, and it is a complex process that affects multiple metabolic pathways after exposure of cells to the toxic substance and as a result, leads to inducing cells to die. Death occurs in the cell either as apoptosis or necrosis, which is usually accompanied by changes in the shape of the nucleus, cell permeability, and mitochondrial functions, which leads to the loss of the function of the mitochondrial membranes and the release of cytochrome C from the mitochondria [16].

There are many studies showing the toxicity of Ag:ZnO nanocomposite made from plant extracts on cancer cells. The Ag:ZnO nanocomposite made from extracts *of Murraya koenigii* and *Zingiber officinale* showed cytotoxicity towards MCF-7 cancer cell line cells by inducing nuclear fragmentation, chromatin condensation and cell entry into programmed death as a result of increased synthesis of free oxygen radicals after treatment and the excretion of virulence. Destroyed mitochondria [16]. In another study, the inhibitory concentration (IC50) value of Ag:ZnO NPs was determined on HaCaT cancer cells, and the IC50 value was 40 µg/ml. Where cells treated with Ag-ZnO NPs for 24 h. showed changes in apoptosis characteristics, including cell shrinkage, nuclear condensation, and breakage, in addition to the formation of apoptotic bodies [17].

## CONFLICT OF INTEREST

The authors declare that there is no conflict of interests regarding the publication of this manuscript.

## REFERENCES


1. Al-Shammari A, Salman M, Saihood Y, Yaseen N, Raed K, Shaker H, et al. In Vitro Synergistic Enhancement of Newcastle Disease Virus to 5-Fluorouracil Cytotoxicity against Tumor Cells. Biomedicines. 2016;4(1):3.
2. Jweer KA, Abed IA, Al-Falahi MNA. The effect of fermentation of organic solid waste with C:N ratios with phosphate rock reinforcement on its biorecycling. Biochemical and Cellular Archives. 2022:3559-3564.
3. Yu MK, Park J, Jon S. Targeting Strategies for Multifunctional Nanoparticles in Cancer Imaging and Therapy. Theranostics. 2012;2(1):3-44.
4. Hassan F, Mohammed G, El-Hiti GA, Alshanon A, Yousif E. Cytotoxic effects of tamoxifen in breast cancer cells. Journal of Unexplored Medical Data. 2018;3(2):3.
5. Giuliano KA, DeBiasio RL, Dunlay RT, Gough A, Volosky JM, Zock J, et al. High-Content Screening: A New Approach to Easing Key Bottlenecks in the Drug Discovery Process. SLAS Discovery. 1997;2(4):249-259.
6. Abraham VC, Towne DL, Waring JF, Warrior U, Burns DJ. Application of a High-Content Multiparameter Cytotoxicity Assay to Prioritize Compounds Based on Toxicity Potential in Humans. SLAS Discovery. 2008;13(6):527-537.
7. Ding GJF, Fischer PA, Boltz RC, Schmidt JA, Colaianne JJ, Gough A, et al. Characterization and Quantitation of NF-κB Nuclear Translocation Induced by Interleukin-1 and Tumor Necrosis Factor-α. J Biol Chem. 1998;273(44):28897-28905.
8. Yashni G, Willy KB, Al-Gheethi AA, Mohamed RMSR, Mohd Salleh SNA, Amir Hashim MK. A Review on Green Synthesis of ZnO Nanoparticles Using Coriandrum Sativum Leaf Extract For Degrading Dyes in Textile Wastewater: A Prospect Towards Green Chemistry. IOP Conference Series: Materials Science and Engineering. 2020;736(4):042003.
9. Saleem M, Ahmed B, Qadir MI, Mahrukh, Rafiq M, Ahmad M, et al. Hepatoprotective effect of Chenopodium murale in mice. Bangladesh Journal of Pharmacology. 2014;9(1).
10. Cannell RJP. Follow-Up of Natural Product Isolation. Methods in Biotechnology: Humana Press; 1998. p. 425-463.
11. Keskin SG, Stanley JM, Mitchell LA, Holliday BJ. Synthesis, characterization, coordination chemistry, and luminescence studies of copper, silver, palladium, and platinum complexes with a phosphorus/nitrogen/phosphorus ligand. Inorg Chim Acta. 2019;486:200-212.
12. Soule HD, Vazquez J, Long A, Albert S, Brennan M. A Human Cell Line From a Pleural Effusion Derived From a Breast Carcinoma 2. JNCI: Journal of the National Cancer Institute. 1973;51(5):1409-1416.
13. Patil SS, Patil RH, Kale SB, Tamboli MS, Ambekar JD, Gade WN, et al. Nanostructured microspheres of silver @ zinc oxide: an excellent impeder of bacterial growth and biofilm. J Nanopart Res. 2014;16(11).
14. Nagaraju G, Udayabhanu, Shivaraj, Prashanth SA, Shastri M, Yathish KV, et al. Electrochemical heavy metal detection, photocatalytic, photoluminescence, biodiesel production and antibacterial activities of Ag–ZnO nanomaterial. Mater Res Bull. 2017;94:54-63.
15. Arumai Selvan DS, keerthi M, Murugesan S, Shobana S, Lakshmi B, Veena V, et al. In vitro cytotoxicity efficacy of phytosynthesized Ag/ZnO nanocomposites using Murraya koenigii and Zingiber officinale extracts. Materials Chemistry and Physics. 2021;272:124903.
16. Rajendran R, Mani A. Photocatalytic, antibacterial and anticancer activity of silver-doped zinc oxide nanoparticles. Journal of Saudi Chemical Society. 2020;24(12):1010-1024.
17. Eleftheriadis T, Pissas G, Liakopoulos V, Stefanidis I. Cytochrome c as a Potentially Clinical Useful Marker of Mitochondrial and Cellular Damage. Front Immunol. 2016;7.
18. Esmekaya MA, Canseven AG, Kayhan H, Tuysuz MZ, Sirav B, Seyhan N. Mitochondrial hyperpolarization and cytochrome-c release in microwave-exposed MCF-7 cells. Gen Physiol Biophys. 2017;36(02):211-218.
19. Borisenko GG. Mitochondrial phospholipid cardiolipin and its triggering functions in the cells. Lipid Technology. 2016;28(2):40-43.